

1

Stereoselective Glycosylations – Additions to Oxocarbenium Ions

Bas Hagen, Stefan van der Vorm, Thomas Hansen, Gijs A. van der Marel, and Jeroen D.C. Codée

1.1 Introduction

Tremendous progress has been made in the construction of oligosaccharides, and many impressive examples of large and complex oligosaccharide total syntheses have appeared over the years [1]. At the same time, the exact mechanism underlying the union of two carbohydrate building blocks often remains obscure, and optimization of a glycosylation reaction can be a time- and labor-intensive process [2, 3]. This can be explained by the many variables that affect the outcome of a glycosylation reaction: the nature of both the donor and acceptor building blocks, solvent, activator and activation protocol, temperature, concentration, and even the presence and the type of molecular sieves. The large structural variety of carbohydrates leads to building blocks that differ significantly in reactivity, with respect to both the nucleophilicity of the acceptor molecule and the reactivity of the donor species. The reactivity of a donor is generally related to the capacity of the donor to accommodate developing positive charge at the anomeric center, upon expulsion of the anomeric leaving group. This also determines the amount of carbocation character in the transition state leading to the products. Most glycosylation reactions will feature characteristics of both S_N1 - and S_N2 -type pathways in the transition states leading to the products. It is now commonly accepted that the exact mechanism through which a glycosidic linkage is formed can be found somewhere in the continuum of reaction mechanisms that spans from a completely dissociative S_N1 mechanism on one side to an associative S_N2 pathway on the other side (Figure 1.1) [4–6]. On the S_N1 -side of the spectrum, glycosyl oxocarbenium ions are found as product-forming intermediates. On this outer limit of the reaction pathway continuum, the oxocarbenium ions will be separated from their counterions by solvent molecules (solvent-separated ion pairs, SSIPs), and there will be no influence of the counterion on the selectivity of the reaction. Moving toward the S_N2 side of the spectrum contact (or close) ion pairs (CIPs) are encountered, and in reactions of these species, the counterion will have a role to play. Because glycosylation reactions generally occur in apolar solvents (dichloromethane is by far the most used one), ionic intermediates have very limited lifetimes, and activated donor species will primarily be present as a pool of

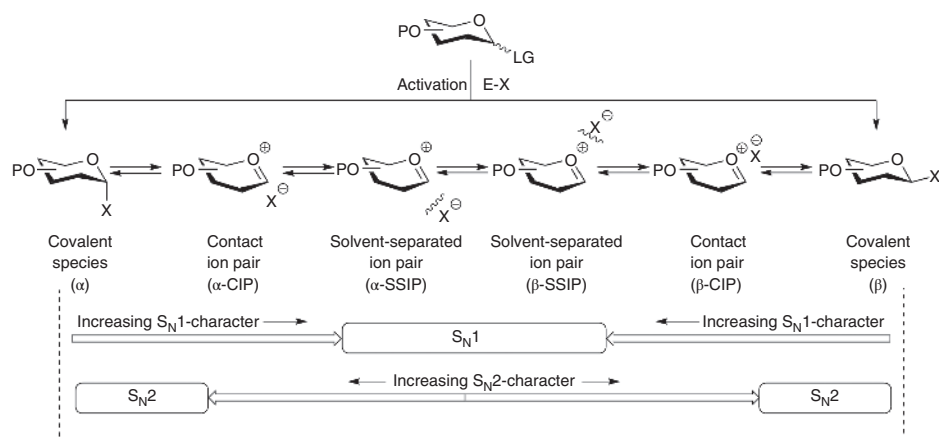
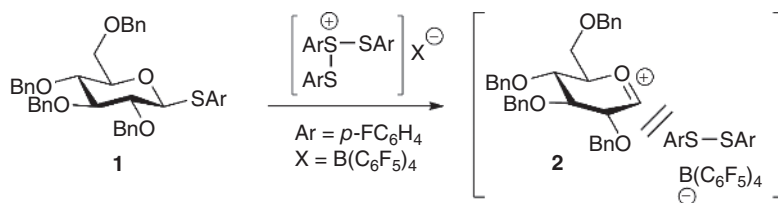


Figure 1.1 Continuum of mechanisms to explain the stereochemical course of glycosylation reactions.

covalent intermediates. The stability, lifetime, and reactivity of an oxocarbenium ion depend – besides the nature of the counterion – on the nature and orientation of the functional groups present on the carbohydrate ring. This chapter explores the role of oxocarbenium ions (and CIPs, featuring a glycosyl cation) in chemical glycosylation reactions. While it was previously often assumed that glycosylations, proceeding via an oxocarbenium ion intermediate, show poor stereoselectivity, it is now clear that oxocarbenium ions can be at the basis of stereoselective glycosylation events. The first part of this chapter deals with the stability, reactivity, and conformational behavior of glycosyl oxocarbenium ions, whereas the second part describes their intermediacy in the assembly of (complex) oligosaccharides.

1.2 Stability, Reactivity, and Conformational Behavior of Glycosyl Oxocarbenium Ions

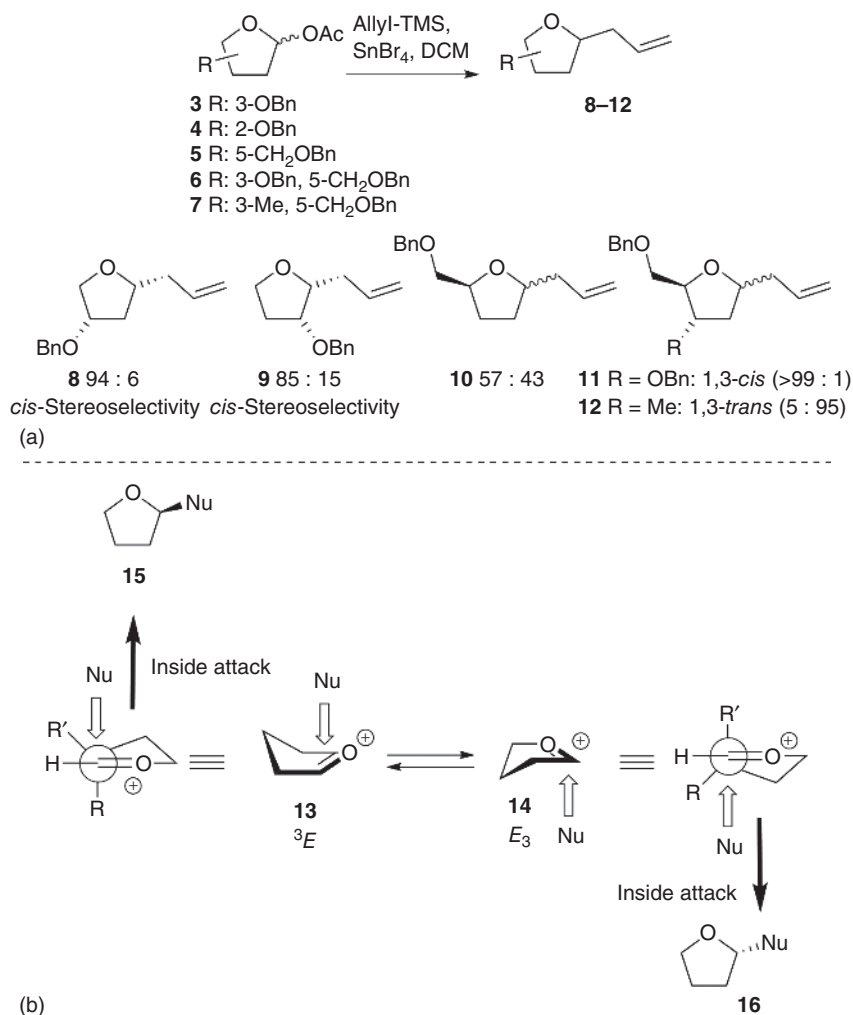
Amyes and Jencks have argued that glycosyl oxocarbenium ions have a short but significant lifetime in aqueous solution [7]. They further argued that in the presence of properly positioned counterions (such as those derived of expulsion of an aglycon), CIPs will rapidly collapse back to provide the covalent species and that the “first stable intermediate for a significant fraction of the reaction” should be the solvent-separated oxocarbenium ion. By extrapolation of these observations to apolar organic solvents, Sinnott reached the conclusion that intimate ion pairs have no real existence in an apolar environment, such as used for glycosylation reactions [8]. Hosoya *et al.* have studied CIPs by quantum mechanical calculations in dichloromethane as a solvent [9]. In these calculations, they have included four solvent molecules to accurately mimic the real-life situation. In many of the studied cases, CIPs turned out to be less stable than the corresponding solvent-separated ions, as will be described next [10]. Yoshida and coworkers have described that activation of thioglucoside **1** with a sulfonium salt activator, featuring the bulky nonnucleophilic tetrakis(pentafluorophenyl) borate counterion, in a continuous-flow microreactor, provides a reactive species (**2**) that has a lifetime on the



Scheme 1.1 Generation of glucosyl oxocarbenium ions in a continuous-flow microreactor.

order of a second (Scheme 1.1) [11]. They argued that this species was a glucosyl oxocarbenium ion, “somewhat stabilized” by the disulfide generated from the donor aglycon and the activator.

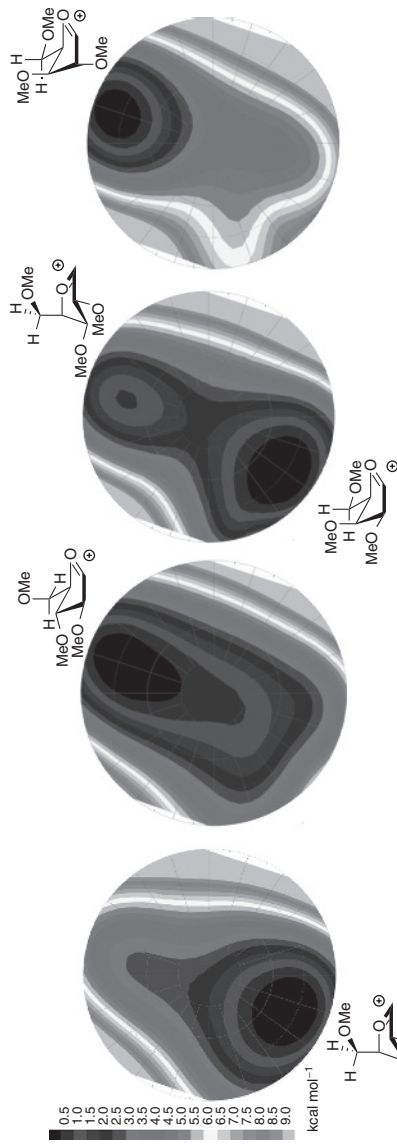
The stability of a glycosyl oxocarbenium ion is largely influenced by the substituents on the carbohydrate ring. The electronegative substituents (primarily oxygen, but also nitrogen-based) have an overall destabilizing effect on the carbocation, and the destabilizing effect can be further enhanced by the presence of electron-withdrawing protecting groups, such as acyl functions. The exact position of the substituent on the ring and its orientation influence the stability of the anomeric cation. The combined influence of all substituents on the ring determines the reactivity of a glycosyl donor, and the extensive relative reactivity value (RRV) charts, drawn up by the Ley and Wong groups for a large panel of thioglycosides, clearly illustrate these functional group effects [12–14]. From these RRV tables, it is clear that the donor reactivity spectrum spans at least eight orders of magnitude. To investigate the influence of the carbohydrate ring substituents on the stereochemical outcome of a glycosylation reaction, Woerpel and coworkers have systematically studied C-glycosylation reactions of a set of furanosides and pyranosides, featuring a limited amount of ring substituents [15–20]. Their studies in the furanose series are summarized in Scheme 1.2a [15, 17]. As can be seen, the alkoxy groups at C2 and C3 have a strong influence on the stereochemical outcome of the reaction, where the alkoxy group at C5 appears to have less effect on the reaction. The presence of an alkoxy or alkyl group at C3 leads to the formation of the allylglycosides **11** and **12** with opposite stereoselectivity. Woerpel and coworkers have devised a model to account for these stereodirecting substituent effects that takes into account the equilibrium between two possible envelope oxocarbenium ion conformers (**13** and **14**, Scheme 1.2b) [17]. Attack on these oxocarbenium ion conformers by the nucleophile occurs from the “inside” of the envelopes, because this trajectory avoids unfavorable eclipsing interactions with the substituent at C2, and it leads, upon rehybridization of the anomeric carbon, to a fully staggered product (**15** and **16**), where attack on the “outside” would provide the furanose ring with an eclipsed C1–C2 constellation. The spatial orientation of the alkoxy groups influences the stability of the oxocarbenium ions. An alkoxy group at C3 can provide some stabilization of the carbocation when it takes up a *pseudo*-axial position. Stabilization of the oxocarbenium ion featuring a C2-alkoxy group is best achieved by placing the electronegative substituent in a *pseudo*-equatorial position to allow for the hyperconjugative stabilization by the properly oriented C2–H2 bond. Alkyl substituents at C3 prefer to adopt a *pseudo*-equatorial position because of steric reasons. With these spatial substituent preferences, the stereochemical outcome of the C-allylation reactions in Scheme 1.2 can be explained. Activation of the C3-benzyloxyfuranosyl acetate with SnBr₄ can provide an



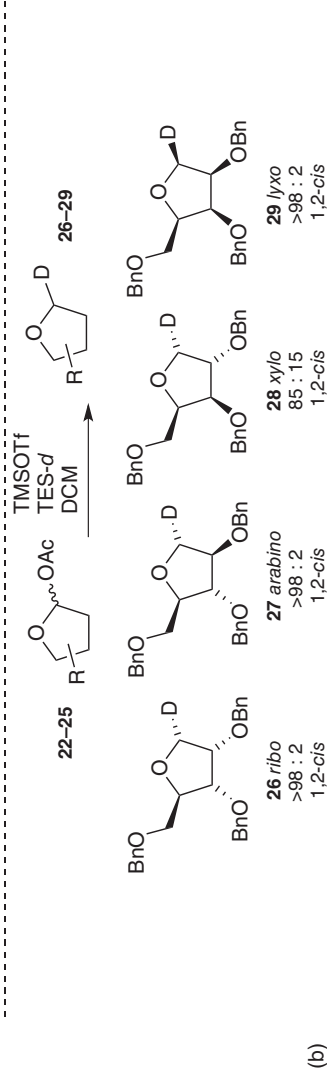
Scheme 1.2 (a) Diastereoselective C-allylations of furanosyl acetates. (b) “Inside” attack model.

oxocarbenium ion intermediate that preferentially adopts an E_3 conformation, as in **14**. Nucleophilic attack on this conformer takes place from the diastereotopic face that leads to the 1,3-*cis* product. In a similar vein, inside nucleophilic attack on the C2-benzyloxy furanosyl oxocarbenium ion E_3 conformer, derived from furanosyl acetate **4**, accounts for the stereochemical outcome of the C-allylation leading to product **9**.

To accurately gauge the combined effect of multiple substituents on a furanosyl ring, van Rijssel *et al.* [21, 22] used a quantum mechanical calculation method, originally developed by Rhoad and coworkers [23], to map the energy of furanosyl oxocarbenium ions related to the complete conformational space they can occupy. Energy maps for all four possible diastereoisomeric, fully decorated furanosyl oxocarbenium ions were generated revealing the lowest energy conformers for the ribo-, arabino-, xylo-, and lyxo-configured furanosyl oxocarbenium ions **17–21** (Scheme 1.3). It became apparent that the orientation of the C5-substituent, having a *gg*, *gt*, or *tg* relation to the substituents at



(a)

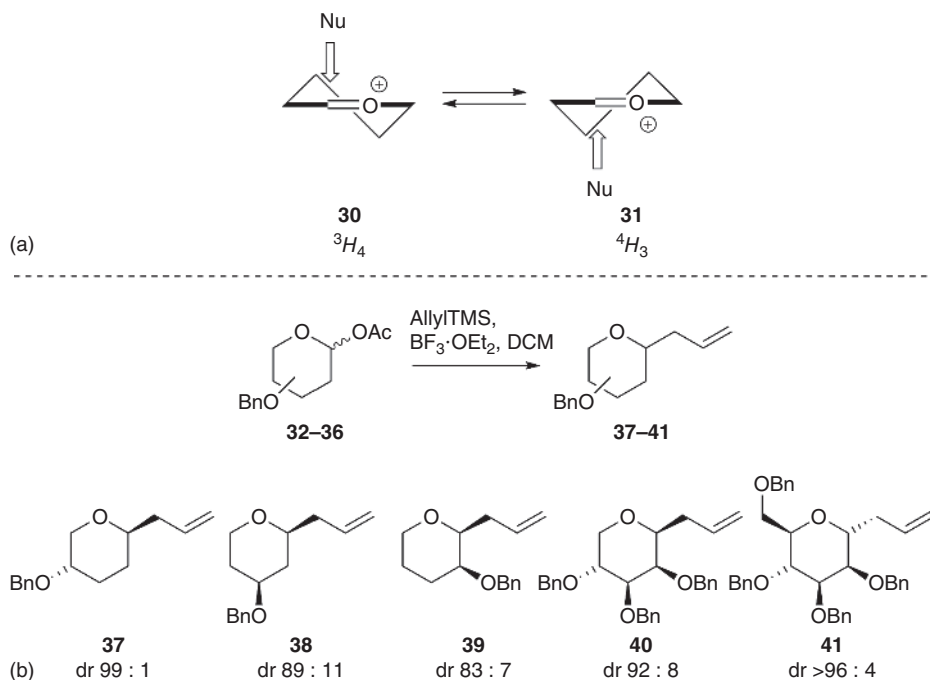


Scheme 1.3 Free energy surface maps of fully decorated furanosyl oxocarbenium ions and diastereoselective reductions of furanosyl acetates.

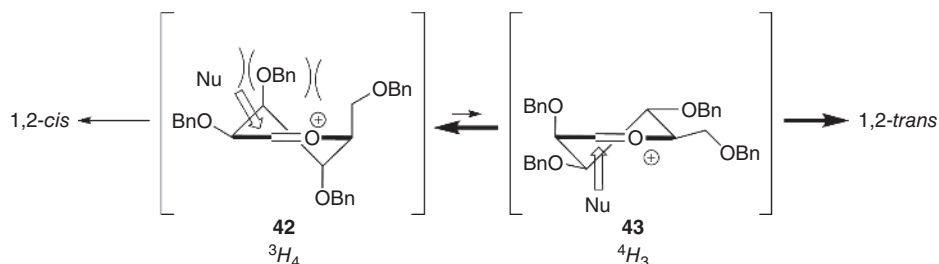
C4, was of profound influence on the stability of the oxocarbenium ions, and differences up to 4 kcal mol^{-1} were observed for structures only differing in their C4–C5 rotation. These stereoelectronic effects have also been described in the pyranose series, where a C4–C6 acetal can restrict the C6-oxygen in a *tg* position, for *manno*- and *gluco*-configured systems, or in a *gg* position for *galacto*-configured constellations [24–26]. The *tg* orientation represents the most destabilizing orientation because in this situation, the O6 atom is farthest away from the electron-depleted anomeric center, not allowing for any electron density donation for stabilization. With the lowest energy furanosyl oxocarbenium ion conformers found by the free energy surface (FES) mapping method, the stereochemical outcome of reduction reactions at the anomeric center of the four diastereoisomeric furanosyl acetates **22–25** could be explained (Scheme 1.3). Interestingly, all four furanosides reacted in a 1,2-*cis* selective manner with the incoming nucleophile (tri-ethylsilane-*d*). Only xylofuranosyl acetate **24** provided some of the 1,2-*trans* addition products, which could be related to the stability of the 3E *gt* oxocarbenium ion intermediate **20**.

The stereoelectronic substituent effects found in the furanose series are paralleled in the pyranose system, where the following substituent effects have been delineated: the stability of pyranosyl oxocarbenium ions benefits from an equatorial orientation of the C2-alkoxy groups (allowing for hyperconjugative stabilization by the $\sigma_{\text{C2-H2}}$ bond) and an axial orientation of the C3 and C4 alkoxy groups [20]. The C5-alkoxymethylene group has a slight preference for an equatorial position because of steric reasons [18]. These substituent preferences have been used to explain the stereochemical outcome of a series of C-allylations, using a two-conformer model. Woerpel and coworkers reasoned that six-membered oxocarbenium ions preferentially adopt a half-chair structure to accommodate the flat $[\text{C1}=\text{O5}]^+$ oxocarbenium ion moiety (Scheme 1.4a) [20]. These half-chair intermediates are attacked by incoming nucleophiles following a trajectory that leads to a chair-like transition state. Thus, attack of a 3H_4 half chair **30** preferentially occurs from the β -face (in the case of a D-pyranoside), where attack on the opposite half chair **31** (the 4H_3) leads to the α -product. With the described spatial substituent preferences and mode of nucleophilic attack, the stereoselectivities in the C-allylation reactions shown in Scheme 1.4b can be accounted for: the C4–OBn is *trans*-directing, where the C3 and C2–O–Bn promote the formation of the *cis*-product. In the lyxopyranosyl oxocarbenium ion, these three substituent preferences can be united, and the allylation of 2,3,4-tri-*O*-benzyl lyxopyranosyl acetate **35** proceeds in a highly stereoselective manner to provide the 1,2-*cis* product **40**.

When a C5 benzyloxymethyl group is added to this system, as in a mannosyl cation, it can be reasoned that the 3H_4 oxocarbenium ion is more stable than its 4H_3 counterpart (see Scheme 1.5): the C2, C3, and C4 groups are all positioned properly to provide maximal stabilization of the electron-depleted anomeric center, and only the C5 substituent, in itself not a powerful stereodirecting group, is not positioned favorably [18]. However, the axial orientation of this group does lead to a significant 1,3-diaxial interaction with the axially positioned C3-alkoxy group. The allylation of mannose proceeds with α -selectivity, indicating that nucleophilic attack on the β -face of the 3H_4 oxocarbenium is not a favorable reaction pathway. To account for this stereochemical outcome, Woerpel and coworkers have suggested a Curtin–Hammett kinetic scenario, in which the two half chairs **42** and **43** are in rapid equilibrium. Attack on the 3H_4 conformer suffers from unfavorable steric interactions between the incoming nucleophile and the



Scheme 1.4 (a) Two-conformer model to explain the stereoselectivity in pyranosyl C-allylations. (b) Observed diastereoselectivity in reactions of (partially) substituted pyranosyl acetates (major products are shown).



Scheme 1.5 The 3H_4 and 4H_3 mannosyl oxocarbenium ions and the trajectories of incoming nucleophiles.

substituents at C3 and C5, in addition to the destabilizing C3—C5 interaction, already present in the system. Attack on the α -face of the 4H_3 oxocarbenium ion, on the other hand, is devoid of these unfavorable steric interactions, making this transition state overall more favorable.

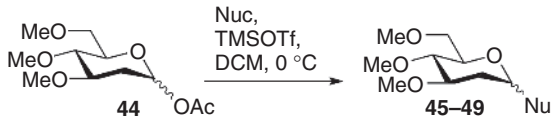
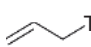
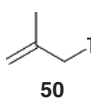
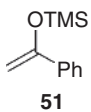
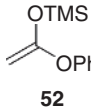
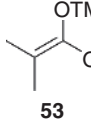
With strong nucleophiles, the two-conformer oxocarbenium ion model falls short, and S_N2 -type pathways come into play [27, 28]. In a continuation of their efforts to understand the stereoselectivities of C-glycosylation reactions of (partially) substituted pyranosyl donors, the Woerpel laboratory studied the addition reactions of a series of C-nucleophiles, ranging from weak nucleophiles (such as allyl trimethylsilane)

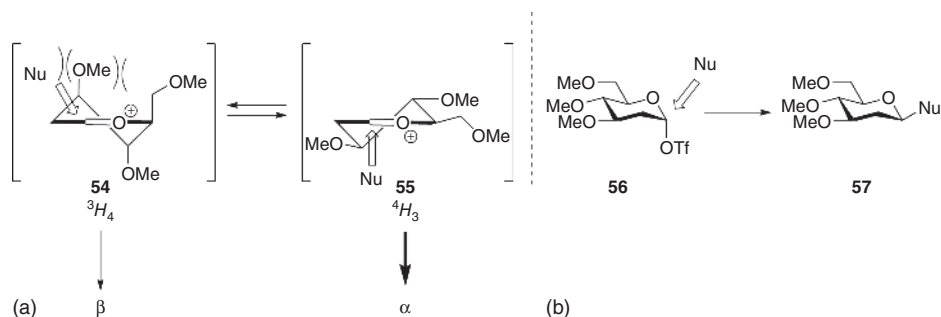
to relatively strong nucleophiles (such as silyl ketene acetals) [27, 28]. Table 1.1 summarizes the stereochemical outcome of the reactions of 2-deoxy glucopyranosyl acetate donor **44** with these nucleophiles under the agency of TMSOTf as a Lewis acid catalyst [28], together with their relative nucleophilicity, as established by Mayr and coworkers [29]. The α -selectivity in the reaction with allyl trimethylsilane can be accounted for by invoking the 4H_3 oxocarbenium ion (**55**, Scheme 1.6a) as most likely product-forming intermediate. Nucleophilic attack on the alternative 3H_4 half chair **54** again suffers from prohibitively large steric interactions to be a reasonable pathway. With reactive nucleophiles, such as silyl ketene acetals **52** and **53** (Table 1.1, entries 4 and 5), the most likely product-forming pathway proceeds with significant S_N2 -character taking place on the α -triflate intermediate **56** (Scheme 1.6b) [28]. Of note, no attempts were undertaken to characterize this triflate[30].

1.3 Computational Studies

To better understand the conformational behavior, reactivity, and stability of glycosyl oxocarbenium ions, several quantum mechanical studies have been undertaken (see Table 1.2) [9, 10, 31–35]. Whitfield and coworkers have reported many computational

Table 1.1 Changing diastereoselectivity in the addition of C-nucleophiles of increasing reactivity.

				
Entry	Nucleophile	N^a	product	α/β (yield)
1		1.8	45	89:11 (57%)
2	 50	4.4	46	50:50 (73%)
3	 51	6.2	47	68:32 (94%)
4	 52	8.2	48	27:73 (78%)
5	 53	9.0	49	19:81 (68%)



Scheme 1.6 Reactive intermediates in S_N1 -type (a) and S_N2 -type (b) pathways.

studies in which they investigated the conformational behavior of, among others, tetra-*O*-methyl gluco- and mannopyranosyl triflates as well as their 4,6-*O*-benzylidene congeners upon ionization (i.e., expulsion of the triflate leaving group) and the conformational behavior of the resulting oxocarbenium ions [32]. To prevent collapse of the initially formed ion pair, they used lithium cations to stabilize the departing anionic leaving

Table 1.2 A selection of oxocarbenium ions and their calculated energies (determined by DFT calculations).

Whitfield	Hosoya CIPs	Hosoya SSIP
tetra-O-Me Glc		
58 (4H_3)	63 (2H_3)	71 (2S_0)
59 (4E)	64 (E_3)	72 (4H_3)
	65 (4H_3) +10.6 kcal mol ⁻¹	
tetra-O-Me Man		
60 (4H_3)	66 (3H_2)	73 (4H_3)
	67 (0S_2) +11.1 kcal mol ⁻¹	74 (0S_2)
Benzylidene-Glc		
61 (4E)	68 (4E)	75 (4E)
Benzylidene-Man		
62 ($B_{2,5}$)	69 ($B_{2,5}$)	76 (1S_0)
	70 ($B_{2,5}$) +14.3 kcal mol ⁻¹	77 ($B_{2,5}$)

group. These calculations revealed that ionization of the tetra-*O*-methyl gluco- and mannopyranosyl α -triflates initially provides 4H_3 (**58** and **60**, respectively) or closely related 4E -like oxocarbenium ions **59** (see Stoddart's hemisphere representation [36] for *pseudo*-rotational itineraries shown in Figure 1.2a). Expulsion of the anomeric triflate from the β -isomers requires a conformational change, where the glucose and mannose pyranosyl rings distort to an 1S_3 -like structure [32]. In this constellation, the anomeric leaving group can be expelled by assistance of one of the ring oxygen lone pairs leading to an 4E (for the glucose) or 4H_3 half-chair (for the mannose) oxocarbenium ion. The stability of these ions is primarily governed by sterics, since they lack the electronic stabilization described earlier. Interestingly, similar itineraries have been established to be operational in glycosyl hydrolases. Rovira and coworkers have determined that the hydrolysis of β -glucosides by retaining glucosyl hydrolases, belonging to the GH5, GH7, and GH16 families, proceeds via a trajectory, in which the substrate is first placed in a conformation that allows expulsion of the aglycon (Figure 1.2b) [37, 38]. Then passing through 4H_3 transition state **80**, which is close in conformational space to the starting 1S_3 geometry **79**, the 4C_1 product **81** (the covalent enzyme–glucose adduct) is obtained. This catalytic itinerary was visualized using a combination of X-ray crystallography, free-energy landscape mapping (to determine the intrinsically favorable ground-state conformations), and quantum mechanics/molecular mechanics reaction simulations. Further calculations of the Whitfield group showed that the 4,6-*O*-benzylidene glucose

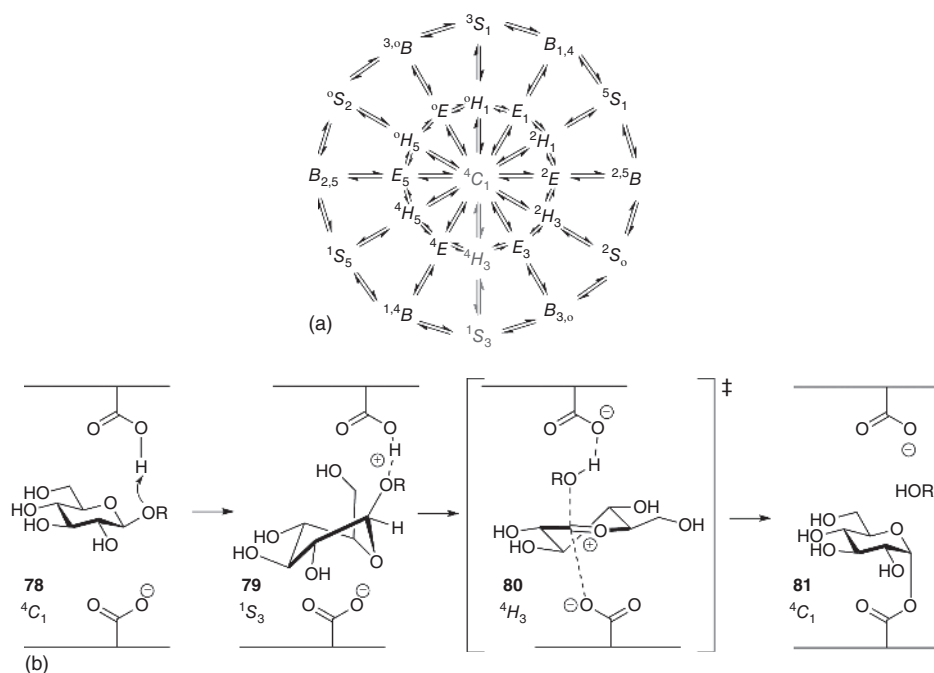


Figure 1.2 (a) Stoddart's hemisphere representation for conformational interconversions (only the Northern hemisphere is shown). (b) Conformational itinerary of the substrate as used by various β -glucosidases. The trajectory has been highlighted in the Stoddart diagram in (a) and was also calculated to be the lowest energy pathway of the ionization of a β -glycosyl triflate.

oxocarbenium ions preferentially take up an 4E conformation **61**, where the corresponding benzyldiene-mannose structure is most stable taking up a $B_{2,5}$ -geometry (**62**) [32]. In the latter structure, both the through-space electron donation by the C3—O—Me ether and the hyperconjugative stabilization of the σ_{C2-H2} bond contribute to the stability of the ion. Recently, Hosoya *et al.* described a method that takes into account explicit solvent molecules in the determination of the stability of CIPs and solvent-separated oxocarbenium ions [10]. They first optimized the amount of solvent molecules required to obtain a reliable outcome while maintaining acceptable calculation costs, eventually using four dichloromethane molecules as an optimum. Using these solvent molecules, they were able to find the lowest energy CIPs and SSIPs. Stabilization of the developing charge was affected by the proper positioning of the solvent molecules: the hydrogen atoms of the dichloromethane molecules were capable of stabilizing the negative charge at the triflate leaving group, while the electron density around the chloride atoms of the dichloromethane molecules could be used to support the positive charge at the oxocarbenium ion. It was described that the stability of tetra-*O*-methyl glucopyranosyl oxocarbenium ions having a triflate associated at either the α - or β -face was quite similar in energy. The lowest energy oxocarbenium ion having the counterion associated on its α -face was found in a $^2H_3/E_3$ conformation (**63/64**) at $+9.5 \text{ kcal mol}^{-1}$ with respect to the lowest energy α -triflate. The β -CIP **65** took up a 4H_3 structure at $+10.6 \text{ kcal mol}^{-1}$.¹ Interestingly, SSIPs that are lower in energy compared to the CIPs were found. A $^2H_3/^2S_O$ SSIP **71** was found to be the most stable, at $+8.5 \text{ kcal mol}^{-1}$, where 4H_3 ion **72** was found at $+10.6 \text{ kcal mol}^{-1}$. For tetra-*O*-methyl mannose, an α -CIP, with an $^OS_2/^3H_2$ structure (**66/67**), was determined to be the most stable ion pair. Although this oxocarbenium does not benefit from an optimal geometry of the $C=O^+$ moiety, it can be stabilized by the σ_{C2-H2} bond and by electron donation from the *pseudo*-axial substituents at C3 and C4. These authors studied the 4,6-*O*-formylidene gluco- and mannopyranosyl oxocarbenium ion pairs to account for stereoselectivities obtained with benzyldiene glucose and mannose donors (*vide infra*) [31]. For the formylidene glucose system, the lowest energy CIP turned out to be the cation **68** with a $^4E/^4H_3$ structure with the anion associated on its β -face ($+13.2 \text{ kcal mol}^{-1}$ with respect to the lowest energy covalent α -triflate). The lowest energy SSIP was found in an 4E conformation ($+10.9 \text{ kcal mol}^{-1}$), in line with the results of the Whitfield group. Also, for the formylidene mannose ion pairs, the SSIPs were found to be more stable compared to the lowest energy CIPs. A $B_{2,5}$ α -CIP (**69**) was found at $+11.7 \text{ kcal mol}^{-1}$ (with respect to the lowest energy α -triflate), where the lowest β -CIP **70** had an $^1S_5/B_{2,5}$ structure ($+14.3 \text{ kcal mol}^{-1}$). The lowest energy SSIP also took up an $^1S_5/B_{2,5}$ conformation (**76/77**) and was significantly more stable ($+9.8 \text{ kcal mol}^{-1}$). The latter geometry corresponds to the structure found by Whitfield [32].

Hünenberger and coworkers have computationally studied ion pairs derived from tetra-*O*-methylglucosyl triflate in different solvents [39]. Through a series of molecular dynamics and quantum mechanical calculations, they came to the hypothesis that different solvents affect the stability of pairs in a different manner. Their calculations suggest that in acetonitrile, the glucopyranosyl oxocarbenium ion preferentially takes up a $B_{2,5}$ structure, with the counterion associated on the α -face. In 1,4-dioxane, a 4H_3

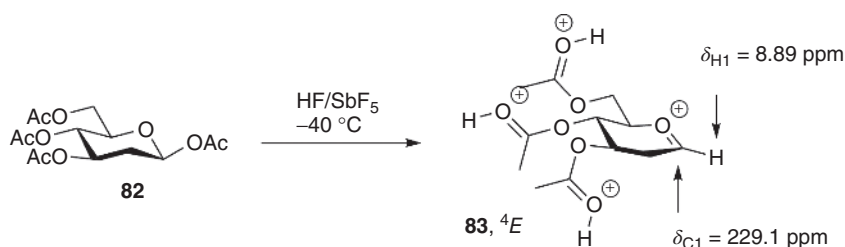
¹ The β -triflate was established to be only $0.8 \text{ kcal mol}^{-1}$ higher in energy compared to its alpha-counterpart, translating to a 3:1 mixture of triflate anomers at equilibrium. Under experimental conditions, only the alpha-anomer has been observed for the tetra-*O*-benzylglucopyranosyl triflate.

structure proved to be most stable with the triflate ion coordinating on the β -face. The authors suggested that their calculations could provide an adequate explanation of the generally observed β - and α -directing effect of the solvents (acetonitrile and 1,4-dioxane, respectively) studied [39].

Because of the different computational approaches, care should be taken to compare the calculation methods described earlier. It is apparent, however, that similarities arise and that the minimum energy conformations determined with the different methods are close in conformational space. For tetra-*O*-benzyl (or methyl) glucose, a structure close to the 4H_3 half chair appears from all calculations. Here, all ring substituents take up a sterically favorable equatorial position. Stabilization of the cation is only provided by hyperconjugation of the C2–H2 bond. For the corresponding mannosyl cation, a similar structure arises, although the method described by Hosoya *et al.* indicates that cations having a rather different structure are also possible [10]. The introduction of a cyclic ketal restricts the conformational freedom of the cations, and the different methods collectively point to an E_4 envelope and $B_{2,5}$ boat structure as most stable oxocarbenium ions for the benzylidene (or formylidene) glucosyl and mannosyl cations, respectively.

1.4 Observation of Glycosyl Oxocarbenium Ions by NMR Spectroscopy

Where many anomeric triflates have been spectroscopically characterized, glycosyl oxocarbenium ions are too reactive to detect by straightforward NMR techniques. Very recently, Blériot and coworkers reported the use of a superacidic medium (HF/SbF₅) to generate glycosyl oxocarbenium ions and allow their spectroscopic investigation [40]. As depicted in Scheme 1.7, 2-deoxyglucosyl donor **82** was transformed into the 4E oxocarbenium ion **83**, which proved to be stable in the super acid medium for several hours at -40°C . The conformation of the ion was deduced from the coupling constants of the ring protons and corroborated by Density Functional Theory calculations and simulated spectra. The found structure is very close in conformational space to the fully substituted glucosyl oxocarbenium ions found in the described DFT calculation (Table 1.2). Quenching of the oxocarbenium ion by cyclohexane-*d*₁₂ led to the selective formation of the α -deuterium 2-deoxy glucoside. The formation of this product can be accounted for by using the 4E oxocarbenium ion as the product-forming

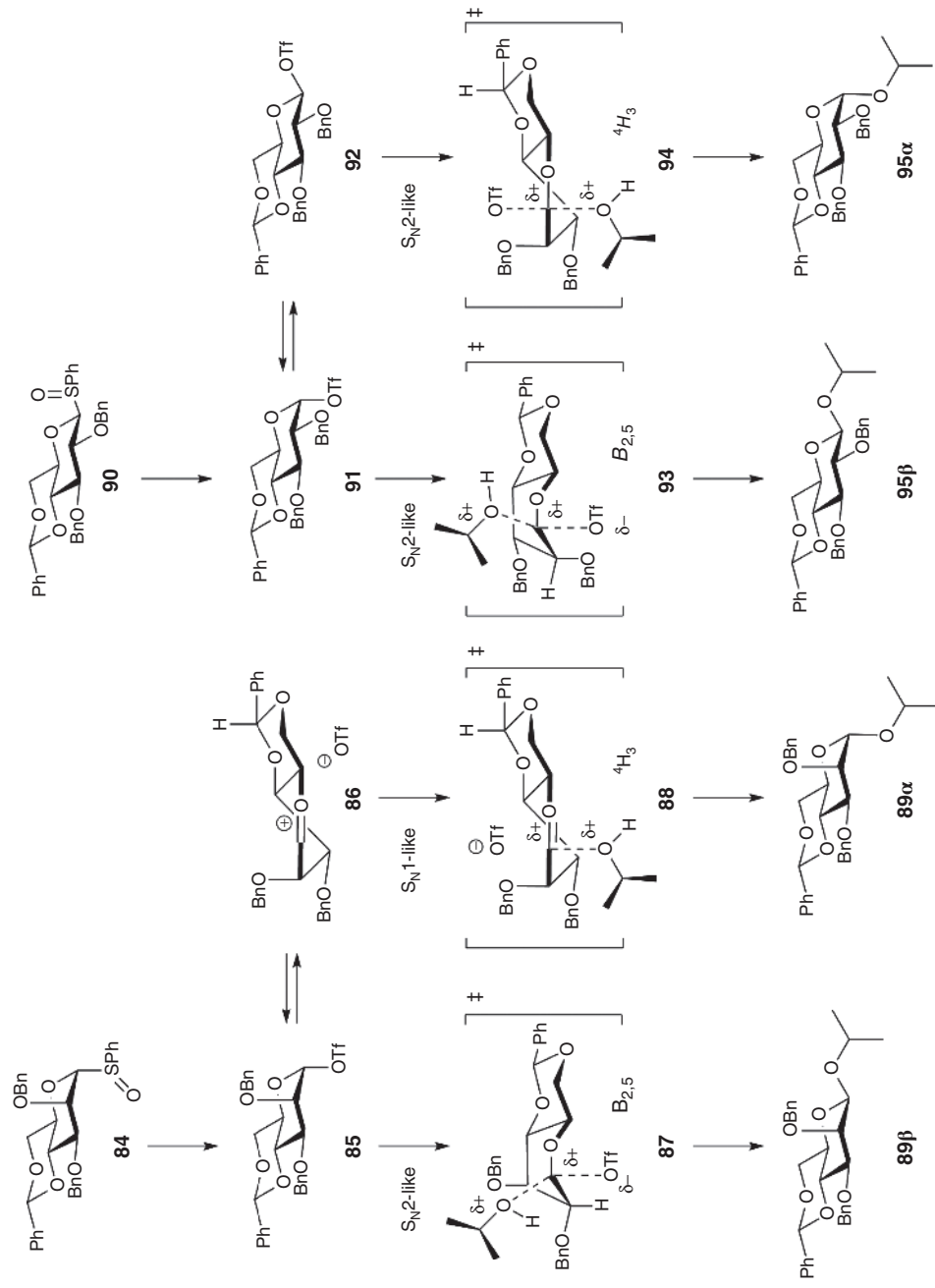


Scheme 1.7 Generation of a 2-deoxy glucosyl oxocarbenium ion in HF/SbF₅ allowing for its characterization by NMR.

intermediate and a favorable ${}^4E \rightarrow {}^4C_1$ reaction trajectory. Obviously, the solvent system used in this NMR experiment differs significantly from the solvents normally used in glycosylation reactions, and, therefore, care should be taken in the translation of the results obtained in the super acid medium to a “normal” glycosylation reaction. It does, however, provide valuable information on the conformation of glycosyl oxocarbenium ions. Expansion of these NMR studies to a broader pallet of carbohydrates with different functionalities will generate insight and spectroscopic proof for stereoelectronic substituent effects that determine the overall shape of the oxocarbenium ions.

1.5 Oxocarbenium Ion(-like) Intermediates as Product-Forming Intermediates in Glycosylation Reactions

The best-studied glycosylation system to date is the Crich β -mannosylation reaction [6, 41–43]. In this reaction (Scheme 1.8), a benzylidene (or related acetal)-protected mannosyl donor (such as **84**) is preactivated to provide an α -anomeric triflate **85**. The corresponding β -triflate is not observed because this species lacks the stabilizing anomeric effect, present in the α -anomer, and it places the anomeric substituent in an unfavorable $\Delta 2$ -position. Addition of an acceptor to the activated donor then provides the β -linked product **89 β** , generally with very high stereoselectivity [44]. While the construction of 1,2-*cis*-mannosides used to be one of the biggest challenges in synthetic carbohydrate chemistry, this linkage can now be installed with great fidelity using this methodology. In addition, the system has been a great inspiration to unravel the underlying mechanistic details to explain the observed stereoselectivity. Crich and coworkers have carried out a suite of studies to understand and learn from the mechanistic pathways operational in the system [45–48]. Secondary kinetic isotope effects, established in a glycosylation reaction with a 2,3,6-tri-*O*-benzyl glucosyl acceptor, revealed significant oxocarbenium ion character in the transition state leading to the β -linked product [45]. This led the authors to presume that the CIP is the actual reactive species in this glycosylation reaction. Using natural abundance ${}^{13}\text{C}$ primary kinetic isotope effects, in combination with computation methods, Crich, Pratt, and coworkers established the amount of carbocation character that develops in the transition state of glycosylations of *iso*-propanol with a benzylidene-protected glucosyl or mannosyl donor [46]. From the established values, corroborated by computational validation, it was established that the β -mannosyl products were formed through an associative pathway, in which the mannose ring adopts a $B_{2,5}$ -structure in the transition state **87**. In contrast, the α -products originated from a more dissociative mechanism, involving a distinct oxocarbenium cation and triflate anion. In this case, computational studies suggested an ${}^4E/{}^4H_3$ structure for the intermediate oxocarbenium ion **86**. For the benzylidene glucose system, which is generally α -selective with carbohydrate acceptors, it was established that both the α - and β -isopropanol products **95 α** and **95 β** were formed through an $\text{S}_{\text{N}}2$ -like mechanism [46]. Notably, upon preactivation of the benzylidene glucose donor, a single triflate is observed: the α -anomer **91** [49]. To account for the formation of the α -product, Crich and coworkers have proposed a Curtin–Hammett kinetic scenario in which the α - and β -triflates **91** and **92** are in rapid equilibrium [46]. Substitution of the most reactive of the two, that is, the β -triflate, then leads to the stereoselectivity observed in reactions of this



Scheme 1.8 Product-forming pathways for benzylidene mannosylations and glucosylations.

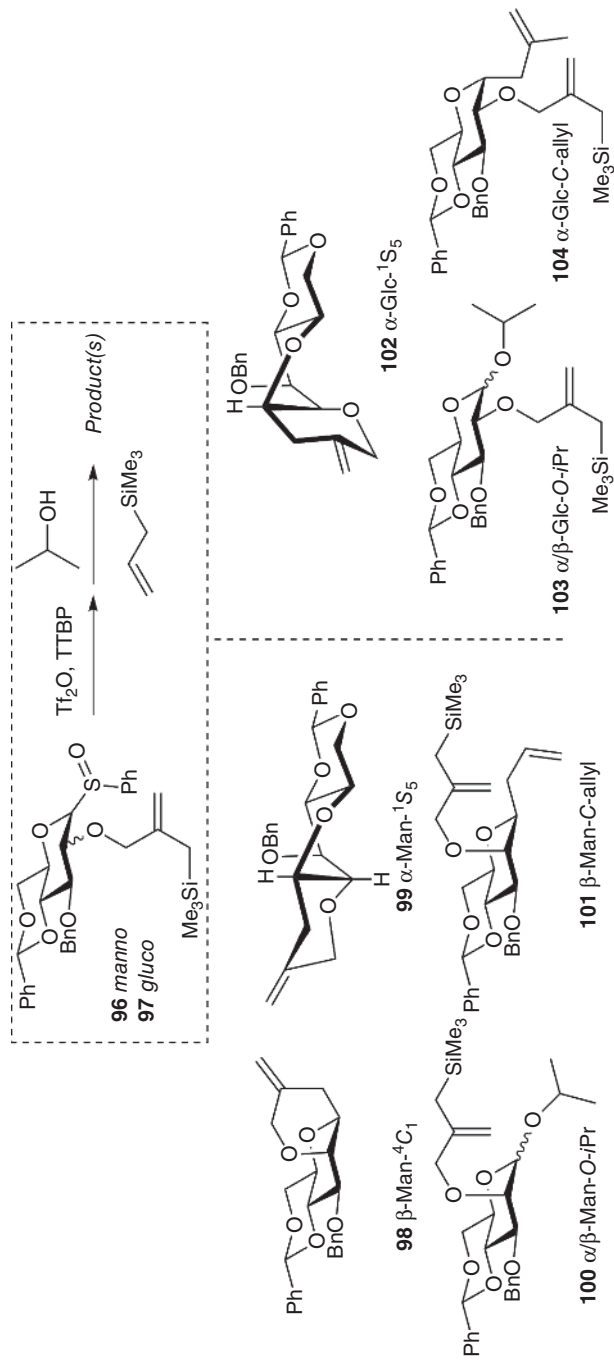
donor. As described next, equatorial glycosyl triflates have been observed, lending support to this scenario [50].

Using the cation clock methodology shown in Scheme 1.9, in which external nucleophiles (isopropanol or allyl trimethylsilane) are made to compete with an intramolecular nucleophile on mannosyl and glucosyl donors **96** and **97** (i.e., an allylsilane ether appended at C2), Crich and coworkers showed the O-glycosylation reactions to be more concentration-dependent compared to the corresponding C-glycosylation reactions [47, 48]. With this methodology, the finding that the formation of the O-glycosyl α - and β -benzylidene products results from different mechanistic pathways (an S_N1 -like pathway for the former and an S_N2 -like pathway for the latter) was corroborated. When trimethyl (methallyl)silane was employed as a nucleophile, only the β -C-allyl mannosyl and α -C-allyl glucosyl products (**101** and **104**, respectively) were obtained in a reaction that was relatively independent of the concentration of the nucleophile, indicating S_N1 -characteristics in these reactions. Of note, formation of the trans-fused benzylidene mannosyl product **99** through intramolecular attack at the α -face indicates the intermediacy of an oxocarbenium ion adopting a $B_{2,5}$ -conformation. The alternative 4H_3 -half chair would not allow the *pseudo*-axially appended nucleophile to reach the α -face of the oxocarbenium ion.

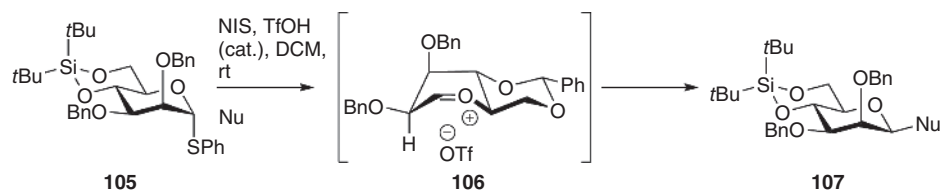
Bols, Pedersen and coworkers have studied glycosylation reactions of the closely related 4,6-*O*-silylidene donor **105** as depicted in Scheme 1.10 [51]. They described that this donor provided the β -linked products with reasonable-to-good selectivity, regardless of the activation protocol (preactivation with BSP/Tf₂O or *in situ* activation with NIS/TfOH). Even when the *in situ* activation method (NIS/TfOH) was employed at room temperature, the β -product formation prevailed. This led the authors to propose the $B_{2,5}$ oxocarbenium ion as the actual reactive species.

The described studies on the benzylidene mannose and glucose systems provide an excellent example of the continuum of mechanisms that operate during a glycosylation reaction. Clearly, the different reaction paths are energetically very close to each other, making a clear-cut distinction between an S_N2 - and an S_N1 -type mechanism impossible. In fact, the structures of the glycosyl donor in the transition state are probably very similar to each other. The analysis presented by Crich and coworkers, as illustrated in Scheme 1.8, shows that the benzylidene mannose ring takes up $B_{2,5}$ -like structure **87** in the S_N2 -displacement of the covalent triflate, where the benzylidene glucose takes up a 4H_3 structure **94** [46]. These structures also represent the conformation of the most stable oxocarbenium ions of these donors. The exact amount of carbocation character in the transition states of these glycosylations will be determined by the difference in timing of the bond-breaking and bond-forming processes. This will critically depend on the nature of the nucleophile. When reactive nucleophiles (such as *iso*-propanol described above) are used, the formation of the new glycosidic linkage will be rather synchronous to the departure of the triflate. Unreactive nucleophiles (such as allyl-TMS and unreactive secondary carbohydrate alcohols) will react through a transition state further along the reaction coordinate, with departure of the triflate preceding the formation of the glycosidic linkage. In this scenario, more positive charge develops at the anomeric center, and the reaction becomes more S_N1 -like.

The C6 oxidized analogs of mannosyl donors, mannuronic acid donors, have been found to be highly β -selective, when both preactivation and direct activation protocols are employed [52–54]. Although it was expected that this type of glycosyl donors would

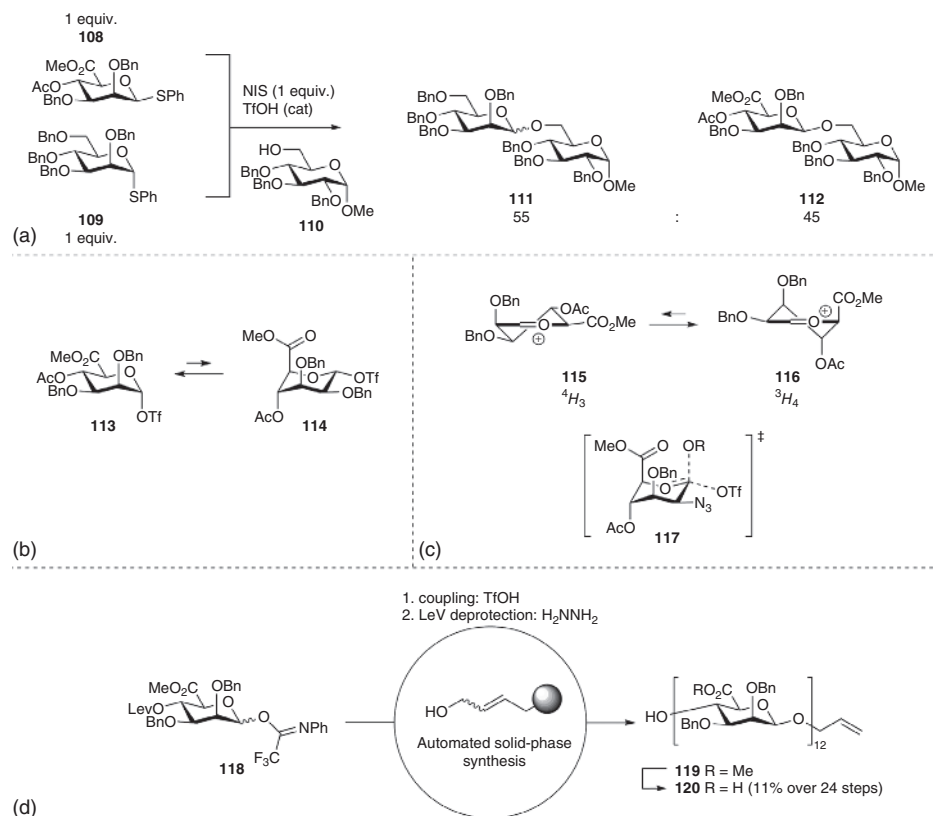


Scheme 1.9 Inter-/intramolecular competition reactions for O- and C-mannosylations and glycosylations.



Scheme 1.10 β -Mannosylation methodology using a 4,6-*O*-silylidene donor.

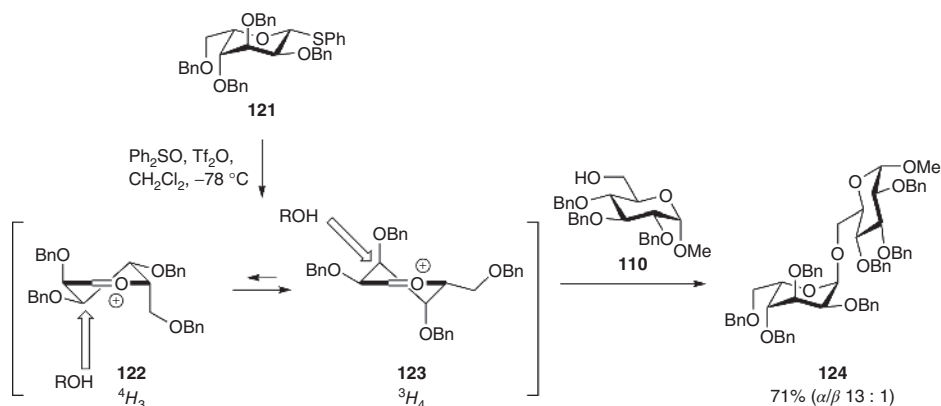
be relatively inactive, by virtue of the electron-withdrawing effect of the C5-carboxylate, these donors turn out to be rather reactive. This is manifested in competition reactions in which the reactivity of mannanuronic acid donor **108** was shown to be in the same order as the reactivity of tetra-*O*-benzyl mannose donor **109** (Scheme 1.11a) [55]. Another illustration of the relatively high reactivity of these species is found in the stability of the anomeric triflates that are formed upon activation of the donors. These are stable up to



Scheme 1.11 Reactivity and selectivity in glycosylation of mannuronic acids. (a) Mannuronic acid donors are more reactive than expected. (b) Mannuronic acid triflates take up different ring conformations. (c) Mannuronic acid oxocarbenium ions and an exploded transition state leading to the β -mannuronic acid linkage. (d) Automated solid-phase assembly of mannuronic acid alginate fragments.

–40°C, a decomposition temperature, which is below that of the 4,6-*O*-benzylidene mannosyl triflate [50]. Strikingly, low-temperature NMR spectroscopy showed the anomeric triflate derived from mannuronic acid donor **108** to take up two conformations at a low temperature, as both the 4C_1 and 1C_4 chairs products were present at –80°C (**113** and **114**, respectively, see Scheme 1.11b). The “inverted” chair triflate places three of the ring substituents in a sterically unfavorable axial orientation. In addition, this structure places the anomeric triflate in an equatorial position, where it does not benefit from a stabilizing anomeric effect. This striking conformational behavior and the relatively high reactivity of these donors were rationalized by the hand of the structure of the oxocarbenium ion that can form from these donors (Scheme 1.11c). In 3H_4 half chair **116**, the C2, C3, and C4 substituents all take up optimal orientations to stabilize the electron-depleted anomeric center (*vide supra*). Model studies on pyranosides, having a single C5 carboxylate group, revealed that this substituent can provide stabilization of the oxocarbenium ion half chair when placed in a *pseudo*-axial position [53]. Thus, in the mannuronic acid 3H_4 half-chair oxocarbenium ion **116**, all substituents collaborate to stabilize the carbocation. This carbocation can also provide an explanation for the β -selectivity observed in glycosylations of these donors. Attack on the diastereotopic face of the half chair that leads to a transition state with a chair-like structure, that is, the β -face, accounts for this selectivity. The smaller size of the carboxylate in comparison to a methyloxybenzyl appendage, present in mannopyranosides, leads to diminished steric interactions of this group with the C3-substituent and the incoming nucleophile (as in Scheme 1.5) [53]. While the stereoselectivity of 4,6-*O*-benzylidene mannose donors decreased with small substituents (e.g., azides) at C2 and C3, the stereoselectivity of C2-azido and C2, C3-diazido mannuronic acid donors remained intact [56, 57]. We have accounted for this “robust” stereoselectivity by taking into account that both an S_N2 -like substitution of the anomeric α -triflates **113** and **114** and an S_N1 -pathway involving the 3H_4 half-chair oxocarbenium ion **116** lead to the β -product (Scheme 1.11c). To minimize steric interactions in this transition state, the mannuronic acid ring may adopt a closely related 3E -structure. The mannuronic acid donors have been successfully employed in the construction of several bacterial oligosaccharides, as well as in the automated solid-phase synthesis of β -mannuronic acid alginate fragments (Scheme 1.11d) [58]. In the latter synthetic endeavor, mannuronic acid *N*-phenyl trifluoroacetimidate donor **118** was used to construct tetra-, octa-, and dodecasaccharide on a resin that was equipped with a butenediol linker system [59]. All glycosylation reactions were executed at a temperature just below the decomposition temperature of the intermediate triflates to allow for effective glycosylation reactions. The dodecasaccharide **120** was eventually obtained, after cleavage from the resin and saponification of the methyl esters, to allow for a straightforward purification, in 11% yield ($\pm 91\%$ per step).

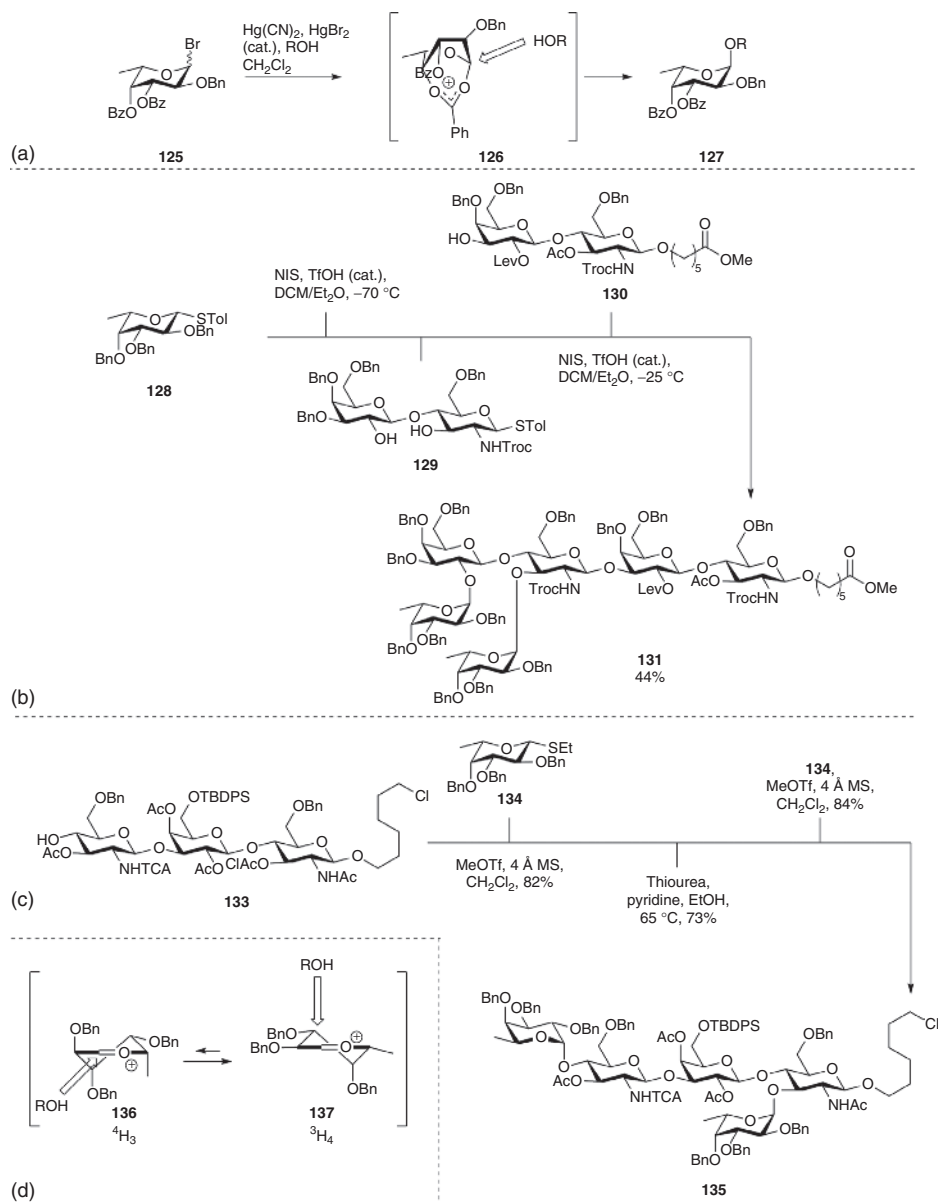
Studies on the C5 epimer of D-mannuronic acid, that is, L-guluronic acid, revealed a marked decrease in 1,2-*cis*-selectivity of these donors [60]. This was explained by taking into account that in the possible L-guluronic acid oxocarbenium ions, there would be conflicting “substituent interests”: in the possible 3H_4 half chair, the C2, C3, and C4 substituents take up a stabilizing orientation, but the C5 carboxylate is positioned in an unfavorable *pseudo*-equatorial orientation. This situation is reversed in the opposite 4H_3 half chair. L-Gulose donors, such as 2,3,4,6-tetra-*O*-benzyl-L-gulosyl donor **121**, on the other hand, provide very selective glycosylation reactions also in the absence of any special stereodirecting functionalities (Scheme 1.12) [60]. In this case, the 3H_4 half-chair



Scheme 1.12 Stereoselective glycosylation involving L-gulosyl donors.

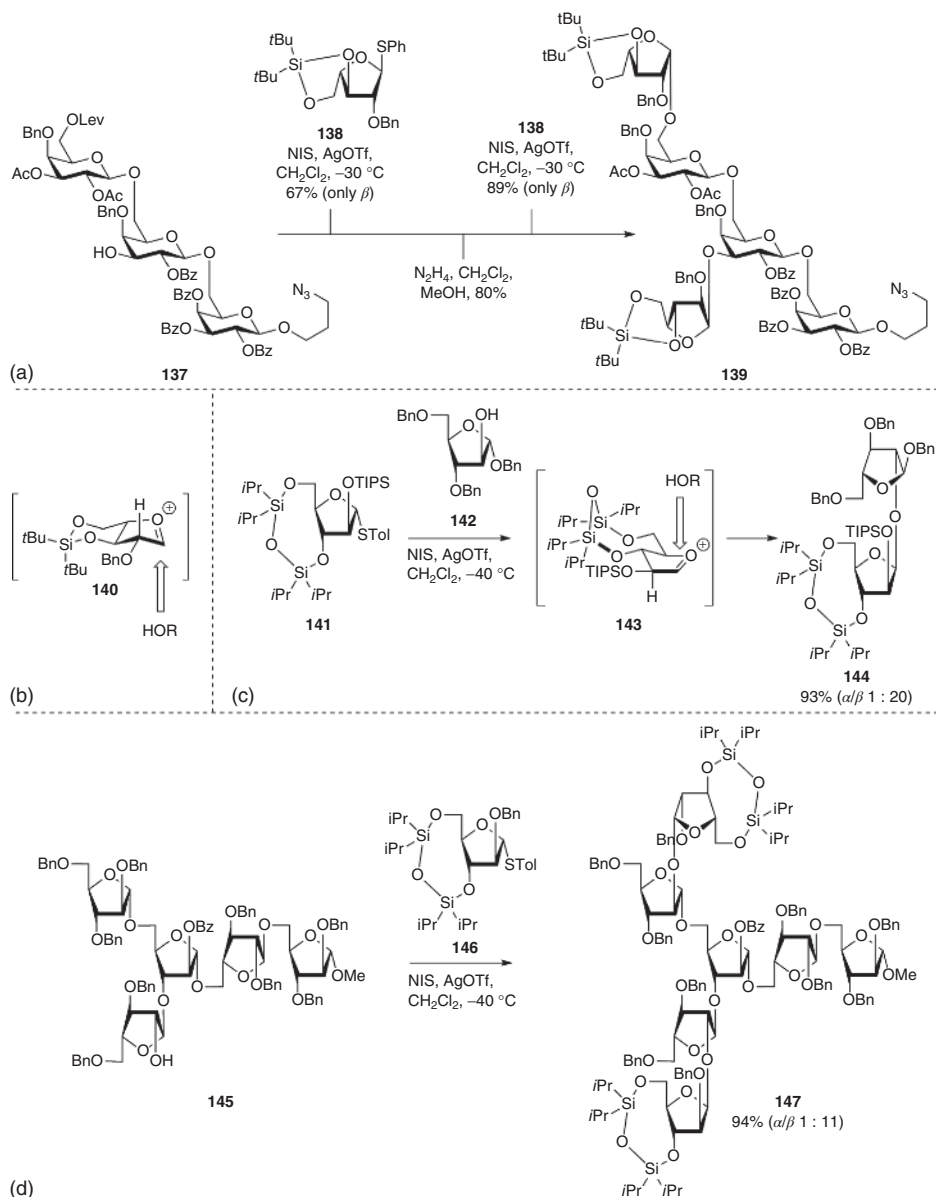
oxocarbenium ion **123** represents a structure that benefits from the stabilization by the functionality at C2, C3, and C4, while minimizing steric interactions between the substituents (especially, the bulky C5 substituent). “Nonoxidized” gulose synthons have been successfully employed in the synthesis of L-guluronic acid alginates [60, 61], as well as “mixed” alginates, containing both β -D-mannuronic acid and α -L-guluronic acid residues [62].

Another L-sugar, renowned for its high 1,2-*cis*-selectivity in glycosylation reactions, is L-fucose, an important constituent of, among others, the blood group determinants [63]. Different methods are available for the introduction of the α -fucosyl linkage. One of the most common methods relies on the use of acyl groups at C3 and/or C4. Although there is ongoing debate on the role of the acyl functions, an often forwarded cited explanation is that they can provide “remote participation,” generating species such as dioxolenium ion **126**, thereby shielding the bottom face of oxocarbenium ion and allowing the selective formation of the α -fucosidic linkage (see Scheme 1.13a) [64–66]. This approach has been successfully employed in the synthesis of fucoidan oligosaccharides [66, 67]. On the other hand, there are also numerous examples of fucosylation that do not rely on the presence of acyl groups at C3 and/or C4. For example, the highly reactive per-*O*-benzylated fucosyl donor **128** has been used by Wong and coworkers to synthesize Lewis^x hapten **131**, using a sequential reactivity-based one-pot strategy, in 44% yield (Scheme 1.13b) [14]. Although the use of the ethereal solvent mixture in this case can be important to install the α -fucosyl linkage, this is most likely not the only reason underlying the excellent selectivity observed in this glycosylation. Another example is shown in Scheme 1.13c where two fucose moieties have been introduced to synthesize pentasaccharide **134**, using perbenzylated thioethyl fucosyl donor **133**, in combination with methyl triflate (MeOTf), in dichloromethane at room temperature [68]. A possible explanation for the generally good α -selectivity observed in fucosylation reactions can be found in oxocarbenium ion half chair **136** (Scheme 1.13d). In this 3H_4 half-chair oxocarbenium ion, the axial C4 alkoxy substituent and the *pseudo*-equatorial H-2 can stabilize the positive charge of the oxocarbenium ion. The C5 methyl substituent is placed in a sterically favorable equatorial position. The high reactivity of perbenzylated fucosyl donors also supports the intermediacy of an oxocarbenium ion intermediate.



Scheme 1.13 (a) Remote participation to explain the α -selectivity of C4-acyl fucosyl donors. (b) Reactivity-based one-pot synthesis of a Lewis^y hexasaccharide using perbenzylated fucosyl thioglycosides. (c) MeOTf-promoted α -fucosylation in the synthesis of a Lewis^a-Lewis^x tumor-associated antigen. (d) Possible half-chair oxocarbenium ions involved in fucosylation reactions.

The use of cyclic protecting groups to conformationally restrict glycosyl donors has also been employed in furanosylation reactions. Almost simultaneously, the Ito, Boons, and Crich groups reported that locked arabinofuranoses can be used for the stereoselective construction of the β -arabinose bond [69–71]. Scheme 1.14a depicts the



Scheme 1.14 Stereoselective arabinofuranosylations through the use of locked arabinofuranosyl donors. (a) Boons' synthesis of an arabinogalactan heptasaccharide. (b) Possible envelope oxocarbenium ions involved in arabinosylation reactions. (c) Ito's conformationally locked arabinoses to achieve high β-selectivities. (d) Ito's synthesis of oligo-arabinofuranosides.

synthesis of an arabinogalactan using 3,5-O-silylidene-protected arabinose donor **137** as reported by Boons and coworkers [70]. The high selectivity of donor **137** was rationalized by the intermediacy of oxocarbenium ion **139** (Scheme 1.14b), which is locked in the E₃ conformation by the cyclic protecting group. The “inside attack” model, described

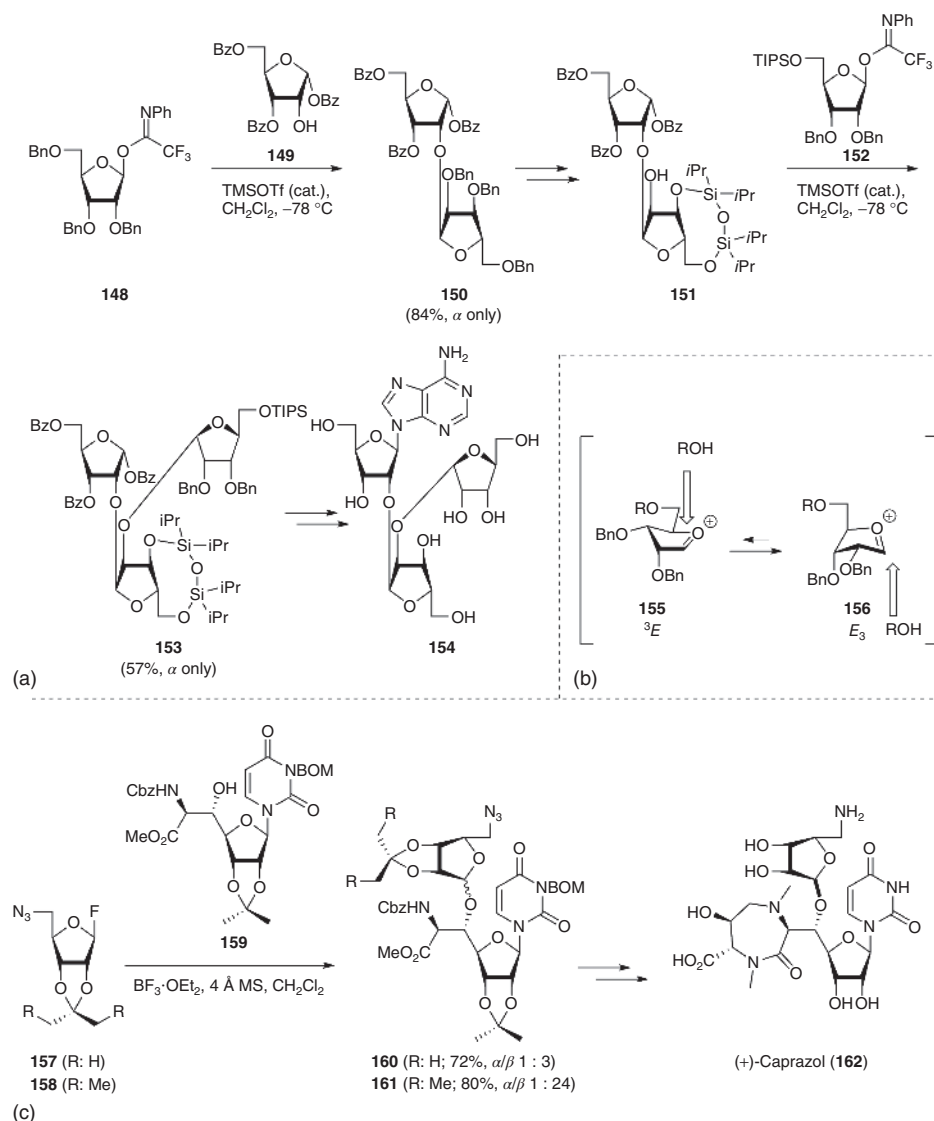
earlier, explains the facial selectivity for the attack of the incoming nucleophile. Ito and coworkers used a similar 3,5-*O*-di-(di-*iso*-propyl)siloxane-protected arabinosyl donor **140** (Scheme 1.14c), which also exhibits a very high β -selectivity [71]. The authors performed molecular modeling studies, which suggested that the total energy of β -glycosylation product **143** was about $3.7 \text{ kcal mol}^{-1}$ lower than that of the alternative α -isomer. The β -glycosidic linkages take up a *pseudo*-axial orientation, thereby benefiting from a stabilizing anomeric effect and providing an explanation for the energy difference. Although the conditions used by the authors do not suggest thermodynamic control in these glycosylations, the energy difference of the products can already become somewhat apparent in the transition states leading to the products. A kinetic explanation for the observed selectivity based on the intermediate oxocarbenium ions is more likely. Analogous donor **145** was used for the introduction of terminal β -arabinofuranosidic residues in branched arabinan oligosaccharides (Scheme 1.14d), up to 22 monosaccharide units in length [71].

As described earlier, C-glycosylation reactions and reductions (addition of an *H*-nucleophile) on ribofuranosides generally proceed with excellent stereoselectivity to provide the product, resulting from nucleophilic attack at the α -face of the E_3 oxocarbenium ion [21]. Also, with other nucleophiles, this stereoselectivity is observed as described in Scheme 1.15a [72]. In their efforts to synthesize poly-(adenosine diphosphate-ribose) trisaccharide core **153** (a so-called supernucleoside), Kistemaker *et al.* used tribenzylated ribosyl donor **147** to form diriboside **149** in high yield and with complete α -selectivity [72]. Further elaboration on the trisaccharide was carried out with 5-*O*-TIPS-protected ribosyl donor **151**, leading to trisaccharide **152**, again with complete α -selectivity, in 57% yield.

The stereoselectivity of ribosyl donors can be reversed through the use of cyclic protecting groups to mask the bottom face of the ribofuranosyl oxocarbenium ion. Ichikawa *et al.* found that 2,3-*O*-(3-pentylidene)-protected ribosyl fluoride **157** reacted in a very β -selective manner with *C*-nucleophiles (Scheme 1.15b) [73, 74]. DFT computations showed that the intermediate oxocarbenium ion preferably adopts an E_3 conformation. Inside attack on this species is prohibited by the blocking 3-pentylidene-protecting group, leading to attack on the other side of the furanosyl ring. This approach was used in the total synthesis of the antibiotic (+)-caprazol **161** (Scheme 1.15c), where 2,3-*O*-(3-pentylidene)-5-azidoribosyl donor **157** gave near-complete β -selectivity in the glycosylation with acceptor **158**, while the less sterically demanding 2,3-*O*-propylidene analog **156** only gave modest β -selectivity [73].

1.6 Conclusion

The vast majority of glycosylation reactions take place somewhere along the continuum of mechanisms hemmed in between S_N1 - and S_N2 -type reactions, with product-forming transition states that have characteristics of both reaction types. Insight into and control over the place of a given glycosylation reaction in the continuum open up ways to control the stereochemical outcome of the glycosylation reaction at hand. Over the recent years – and spurred by the initial discovery of a covalent mannosyl triflate – much insight into reactive intermediates has been gathered. NMR spectroscopy has been used to characterize a multitude of covalent reactive intermediates such as anomeric



Scheme 1.15 Stereoselective ribosylations. (a) Synthesis of the "supernucleoside" **153**. (b) Possible envelope oxocarbenium ions involved in ribosylations. (c) Matsuda's total synthesis of (+)-caprazol **161**.

triflates. Often, only a single anomeric triflate can be observed spectroscopically, because the other anomer is highly unstable to allow its detection. To study glycosyl oxocarbenium ions, sophisticated and detailed DFT computational approaches have been presented to validate the experimental results. Very recently, NMR was added to the toolbox available to study glycosyl oxocarbenium ions. To pinpoint, the location of the mechanism of a given glycosylation reaction on the continuum of mechanisms, kinetic isotope effects, and cation clock methodology have been used to determine how much oxocarbenium character develops in the transition state of the glycosylation

reaction. While the structure of noncharged covalent intermediates is primarily dictated by the steric requirements of the ring substituents, the shape of positively charged oxocarbenium-ion-like intermediates is governed by electronic (stabilizing or destabilizing) substituent effects. These effects will also be apparent in the transition state of a glycosylation reaction in which partial oxocarbenium ion character develops. The amount of positive charge at the anomeric center that can or has to develop for a given glycosylation reaction to occur depends not only on the nature of the donor but also on the nucleophilicity of the acceptor. Acceptors of high nucleophilicity will be able to displace covalent reactive intermediates, where poor nucleophiles require more oxocarbenium ion character. With the ever-growing insight into the reactivity of different reactive intermediates at play during a glycosylation reaction, more control over the stereoselective construction of glycosidic bonds will be gained, reducing the time- and labor-intensive trial-and-error component that has thwarted synthetic carbohydrate chemistry for so long.

References

- 1 (a) Zhu, X. and Schmidt, R.R. (2009) *Angew. Chem. Int. Ed.*, 48, 1900–1934; (b) Werz, D.B. and Seeberger, P.H. (2007) *Nature*, 446, 1046–1051; (c) Boltje, T.J., Buskas, T., and Boons, G.-J. (2009) *Nat. Chem.*, 1, 611–622.
- 2 Demchenko, A.V. (2008) *Handbook of Chemical Glycosylation: Advances in Stereoselectivity and Therapeutic Relevance*, Wiley-VCH Verlag GmbH.
- 3 Nigudkar, S.S. and Demchenko, A.V. (2015) *Chem. Sci.*, 6, 2687–2704.
- 4 Bohé, L. and Crich, D. (2011) *C.R. Chim.*, 14, 3–16.
- 5 Bohé, L. and Crich, D. (2015) *Carbohydr. Res.*, 403, 48–59.
- 6 Crich, D. (2010) *Acc. Chem. Res.*, 43, 1144–1153.
- 7 Amyes, T.L. and Jencks, W.P. (1989) *J. Am. Chem. Soc.*, 111, 7888–7900.
- 8 Sinnott, M.L. and Jencks, W.P. (1980) *J. Am. Chem. Soc.*, 102, 2026–2032.
- 9 Hosoya, T., Takano, T., Kosma, P., and Rosenau, T. (2014) *J. Org. Chem.*, 79, 7889–7894.
- 10 Hosoya, T., Kosma, P., and Rosenau, T. (2015) *Carbohydr. Res.*, 401, 127–131.
- 11 Saito, K., Ueoka, K., Matsumoto, K., Suga, S., Nokami, T., and Yoshida, J. (2011) *Angew. Chem. Int. Ed.*, 50, 5153–5156.
- 12 Douglas, N. L., Ley, S. V., Lücking, U., Warriner, S. L. (1998) *J. Chem. Soc.*, 51–66.
- 13 Zhang, Z., Ollmann, I.R., Ye, X.-S., Wischnat, R., Baasov, T., and Wong, C.-H. (1999) *J. Am. Chem. Soc.*, 121, 734–753.
- 14 Mong, K.-K.T. and Wong, C.-H. (2002) *Angew. Chem.*, 114, 4261–4264.
- 15 Larsen, C.H., Ridgway, B.H., Shaw, J.T., and Woerpel, K.A. (1999) *J. Am. Chem. Soc.*, 121, 12208–12209.
- 16 Shaw, J.T. and Woerpel, K.A. (1999) *Tetrahedron*, 55, 8747–8756.
- 17 Larsen, C.H., Ridgway, B.H., Shaw, J.T., Smith, D.M., and Woerpel, K.A. (2005) *J. Am. Chem. Soc.*, 127, 10879–10884.
- 18 Lucero, C.G. and Woerpel, K.A. (2006) *J. Org. Chem.*, 71, 2641–2647.
- 19 Romero, J.A.C., Tabacco, S.A., and Woerpel, K.A. (2000) *J. Am. Chem. Soc.*, 122, 168–169.
- 20 Ayala, L., Lucero, C.G., Romero, J.A.C., Tabacco, S.A., and Woerpel, K.A. (2003) *J. Am. Chem. Soc.*, 125, 15521–15528.

- 21 van Rijssel, E.R., van Delft, P., Lodder, G., Overkleef, H.S., van der Marel, G.A., Filippov, D.V., and Codée, J.D.C. (2014) *Angew. Chem. Int. Ed.*, 53, 10381–10385.
- 22 van Rijssel, E.R., van Delft, P., van Marle, D.V., Bijvoets, S.M., Lodder, G., Overkleef, H.S., van der Marel, G.A., Filippov, D.V., and Codée, J.D.C. (2015) *J. Org. Chem.*, 80, 4553–4565.
- 23 Rhoad, J.S., Cagg, B.A., and Carver, P.W. (2010) *J. Phys. Chem. A*, 114, 5180–5186.
- 24 Jensen, H.H., Nordstrøm, L.U., and Bols, M. (2004) *J. Am. Chem. Soc.*, 126, 9205–9213.
- 25 Frihed, T.G., Walvoort, M.T.C., Codée, J.D.C., van der Marel, G.A., Bols, M., and Pedersen, C.M. (2013) *J. Org. Chem.*, 78, 2191–2205.
- 26 Moumé-Pymbock, M., Furukawa, T., Mondal, S., and Crich, D. (2013) *J. Am. Chem. Soc.*, 135, 14249–14255.
- 27 Krumper, J.R., Salamant, W.A., and Woerpel, K.A. (2008) *Org. Lett.*, 10, 4907–4910.
- 28 Krumper, J.R., Salamant, W.A., and Woerpel, K.A. (2009) *J. Org. Chem.*, 74, 8039–8050.
- 29 Mayr, H., Bug, T., Gotta, M.F., Hering, N., Irrgang, B., Janker, B., Kempf, B., Loos, R., Ofial, A.R., Remennikov, G. *et al.* (2001) *J. Am. Chem. Soc.*, 123, 9500–9512.
- 30 Frihed, T.G., Bols, M., and Pedersen, C.M. (2015) *Chem. Rev.*, 115, 4963–5013.
- 31 Hosoya, T., Kosma, P., and Rosenau, T. (2015) *Carbohydr. Res.*, 411, 64–69.
- 32 Whitfield, D.M. (2007) *Carbohydr. Res.*, 342, 1726–1740.
- 33 Whitfield, D.M. (2012) *Carbohydr. Res.*, 356, 180–190.
- 34 Whitfield, D.M. (2015) *Carbohydr. Res.*, 403, 69–89.
- 35 Satoh, H. and Nukada, T. (2014) *Trends Glycosci. Glycotechnol.*, 26, 11–27.
- 36 Stoddard, J.F. (1971) *Stereochemistry of Carbohydrates*, Wiley-Interscience, Toronto.
- 37 Ardèvol, A., Biarnés, X., Planas, A., and Rovira, C. (2010) *J. Am. Chem. Soc.*, 132, 16058–16065.
- 38 Davies, G.J., Planas, A., and Rovira, C. (2012) *Acc. Chem. Res.*, 45, 308–316.
- 39 Satoh, H., Hansen, H.S., Manabe, S., van Gunsteren, W.F., and Hünenberger, P.H. (2010) *J. Chem. Theory Comput.*, 6, 1783–1797.
- 40 Martin, A., Arda, A., Désiré, J., Martin-Mingot, A., Probst, N., Sinaÿ, P., Jiménez-Barbero, J., Thibaudeau, S., and Blériot, Y. (2015) *Nat. Chem.* 8, 186–191.
- 41 Crich, D. and Sun, S. (1996) *J. Org. Chem.*, 61, 4506–4507.
- 42 El Ashry, E.S.H., Rashed, N., and Ibrahim, E.S.I. (2005) *Curr. Org. Synth.*, 2, 175–213.
- 43 Yang, L., Qin, Q., and Ye, X.-S. (2013) *Asian J. Org. Chem.*, 2, 30–49.
- 44 Crich, D. and Sun, S. (1998) *Tetrahedron*, 54, 8321–8348.
- 45 Crich, D. and Chandrasekera, N.S. (2004) *Angew. Chem.*, 116, 5500–5503.
- 46 Huang, M., Garrett, G.E., Birlirakis, N., Bohé, L., Pratt, D.A., and Crich, D. (2012) *Nat. Chem.*, 4, 663–667.
- 47 Huang, M., Retailleau, P., Bohé, L., and Crich, D. (2012) *J. Am. Chem. Soc.*, 134, 14746–14749.
- 48 Adero, P.O., Furukawa, T., Huang, M., Mukherjee, D., Retailleau, P., Bohé, L., and Crich, D. (2015) *J. Am. Chem. Soc.* 137, 10336–10345.
- 49 Crich, D. and Sun, S. (1997) *J. Am. Chem. Soc.*, 119, 11217–11223.
- 50 Walvoort, M.T.C., Lodder, G., Mazurek, J., Overkleef, H.S., Codée, J.D.C., and van der Marel, G.A. (2009) *J. Am. Chem. Soc.*, 131, 12080–12081.
- 51 Heuckendorff, M., Bendix, J., Pedersen, C.M., and Bols, M. (2014) *Org. Lett.*, 16, 1116–1119.
- 52 van den Bos, L.J., Dinkelaar, J., Overkleef, H.S., and van der Marel, G.A. (2006) *J. Am. Chem. Soc.*, 128, 13066–13067.

- 53 Codée, J.D.C., van den Bos, L.J., de Jong, A.-R., Dinkelaar, J., Lodder, G., Overkleeft, H.S., and van der Marel, G.A. (2009) *J. Org. Chem.*, 74, 38–47.
- 54 van den Bos, L.J., Codée, J.D.C., Litjens, R.E.J.N., Dinkelaar, J., Overkleeft, H.S., and van der Marel, G.A. (2007) *Eur. J. Org. Chem.*, 2007, 3963–3976.
- 55 Walvoort, M.T.C., de Witte, W., van Dijk, J., Dinkelaar, J., Lodder, G., Overkleeft, H.S., Codée, J.D.C., and van der Marel, G.A. (2011) *Org. Lett.*, 13, 4360–4363.
- 56 Walvoort, M.T.C., Lodder, G., Overkleeft, H.S., Codée, J.D.C., and van der Marel, G.A. (2010) *J. Org. Chem.*, 75, 7990–8002.
- 57 Walvoort, M.T.C., Moggré, G.-J., Lodder, G., Overkleeft, H.S., Codée, J.D.C., and van der Marel, G.A. (2011) *J. Org. Chem.*, 76, 7301–7315.
- 58 Walvoort, M.T.C., van den Elst, H., Plante, O.J., Kröck, L., Seeberger, P.H., Overkleeft, H.S., van der Marel, G.A., and Codée, J.D.C. (2012) *Angew. Chem. Int. Ed.*, 51, 4393–4396.
- 59 Andrade, R.B., Plante, O.J., Melean, L.G., and Seeberger, P.H. (1999) *Org. Lett.*, 1, 1811–1814.
- 60 Dinkelaar, J., van den Bos, L.J., Hogendorf, W.F.J., Lodder, G., Overkleeft, H.S., Codée, J.D.C., and van der Marel, G.A. (2008) *Chem. – Eur. J.*, 14, 9400–9411.
- 61 Chi, F.-C., Kulkarni, S.S., Zulueta, M.M.L., and Hung, S.-C. (2009) *Chem. – Asian J.*, 4, 386–390.
- 62 Zhang, Q., van Rijssel, E.R., Walvoort, M.T.C., Overkleeft, H.S., van der Marel, G.A., and Codée, J.D.C. (2015) *Angew. Chem. Int. Ed.*, 54, 7670–7673.
- 63 Storry, J.R. and Olsson, M.L. (2009) *Immunohematology*, 25, 48–59.
- 64 Park, J., Boltje, T.J., and Boons, G.-J. (2008) *Org. Lett.*, 10, 4367–4370.
- 65 Werz, D.B. and Vidal, S. (2013) *Modern Synthetic Methods in Carbohydrate Chemistry: From Monosaccharides to Complex Glycoconjugates*, Wiley VCH, pp. 135–143.
- 66 Gerbst, A.G., Ustuzhanina, N.E., Grachev, A.A., Khatuntseva, E.A., Tsvetkov, D.E., Whitfield, D.M., Berces, A., and Nifantiev, N.E. (2001) *J. Carbohydr. Chem.*, 20, 821–831.
- 67 Gerbst, A.G., Ustuzhanina, N.E., Grachev, A.A., Zlotina, N.S., Khatuntseva, E.A., Tsvetkov, D.E., Shashkov, A.S., Usov, A.I., and Nifantiev, N.E. (2002) *J. Carbohydr. Chem.*, 21, 313–324.
- 68 Guillemineau, M. and Auzanneau, F.-I. (2012) *J. Org. Chem.*, 77, 8864–8878.
- 69 Crich, D., Pedersen, C.M., Bowers, A.A., and Wink, D.J. (2007) *J. Org. Chem.*, 72, 1553–1565.
- 70 Zhu, X., Kawatkar, S., Rao, Y., and Boons, G.-J. (2006) *J. Am. Chem. Soc.*, 128, 11948–11957.
- 71 Ishiwata, A., Akao, H., and Ito, Y. (2006) *Org. Lett.*, 8, 5525–5528.
- 72 Kistemaker, H.A.V., Overkleeft, H.S., van der Marel, G.A., and Filippov, D.V. (2015) *Org. Lett.*, 17, 4328–4331.
- 73 Hirano, S., Ichikawa, S., and Matsuda, A. (2005) *Angew. Chem. Int. Ed.*, 44, 1854–1856.
- 74 Ichikawa, S., Hayashi, R., Hirano, S., and Matsuda, A. (2008) *Org. Lett.*, 10, 5107–5110.